



## FULL LENGTH ARTICLE

# Circulating exosome-like vesicles of humans with nondiabetic obesity impaired islet $\beta$ -cell proliferation, which was associated with decreased Omentin-1 protein cargo

Qian Ge <sup>a,1</sup>, Xinxin Xie <sup>b,1</sup>, Xiangjun Chen <sup>a</sup>, Rongfeng Huang <sup>c</sup>,  
Cheng-Xue Rui <sup>b,d</sup>, Qianna Zhen <sup>a</sup>, Renzhi Hu <sup>a</sup>, Min Wu <sup>c</sup>,  
Xiaoqiu Xiao <sup>c,\*\*,1</sup>, Xi Li <sup>b,\*,1</sup>

<sup>a</sup> Department of Endocrinology, The First Affiliated Hospital of Chongqing Medical University, Chongqing 400016, PR China

<sup>b</sup> The Biology Science Institutes, Chongqing Medical University, Chongqing 400016, PR China

<sup>c</sup> The Chongqing Key Laboratory of Translational Medicine in Major Metabolic Diseases, The First Affiliated Hospital of Chongqing Medical University, Chongqing 400016, PR China

<sup>d</sup> de Duve Institute, Catholic University of Louvain, Brussels 1200, Belgium

Received 8 October 2020; received in revised form 21 December 2020; accepted 27 December 2020  
Available online 2 January 2021

## KEYWORDS

$\beta$ -Cell;  
Exosome;  
Obesity;  
Proliferation;  
Type 2 diabetes mellitus

**Abstract** The regulation of  $\beta$ -cell mass in the status of nondiabetic obesity remains not well understood. We aimed to investigate the role of circulating exosome-like vesicles (ELVs) isolated from humans with simple obesity in the regulation of islet  $\beta$ -cell mass. Between June 2017 and July 2019, 81 subjects with simple obesity and 102 healthy volunteers with normal weight were recruited. ELVs were isolated by ultra-centrifugation. The proliferations of  $\beta$ -cells and islets were measured by 5-ethynyl-2'-deoxyuridine (EdU). Protein components in ELVs were identified by Quantitative Proteomic Analysis and verified by Western blot and ELISA. The role of specific exosomal protein was analyzed by gain-of-function approach in ELVs released by 3T3-L1 preadipocytes. Circulating ELVs from subjects with simple obesity inhibited  $\beta$ -cell proliferation *in vitro* without affecting its apoptosis, secretion, and inflammation. The protein levels of Rictor and Omentin-1 were downregulated in circulating ELVs from subjects with simple obesity and associated with the obesity-linked pathologic conditions. The ELV-carried Omentin-1 and Omentin-1 protein *per se* were validated to increase  $\beta$ -cell proliferation and activate Akt signaling pathway. Moreover, Omentin-1 in ELVs was downregulated by insulin.

\* Corresponding author. No.1 Yixueyuan Road, Yuzhong District, Chongqing 400016, PR China.

\*\* Corresponding author. No.1 Friendship Road, Yuzhong District, Chongqing 400016, PR China.

E-mail addresses: [bshaw2001@163.com](mailto:bshaw2001@163.com) (X. Xiao), [lix@shmu.edu.cn](mailto:lix@shmu.edu.cn) (X. Li).

Peer review under responsibility of Chongqing Medical University.

<sup>1</sup> These authors contributed equally to this work.

The circulating ELVs may act as a negative regulator for  $\beta$ -cell mass in nondiabetic obesity through inhibiting  $\beta$ -cell proliferation. This effect was associated with downregulated Omentin-1 protein in ELVs. This newly identified ELV-carried protein could be a mediator linking insulin resistance to impaired  $\beta$ -cell proliferation and a new potential target for increasing  $\beta$ -cell mass in obesity and T2DM.

Copyright © 2021, Chongqing Medical University. Production and hosting by Elsevier B.V. This is an open access article under the CC BY-NC-ND license (<http://creativecommons.org/licenses/by-nc-nd/4.0/>).

### Abbreviation list

ALT	alanine transaminase
AST	aspartate transaminase
AUC	area under the curve
AUC <sub>INS/G</sub>	insulin secretion index
CCL2	C–C motif ligand 2
CKD4	cyclin dependent kinase 4
Cr	creatinine
EdU	5-ethynyl-2'-deoxyuridine
ELVs	exosomal-like vesicles
FC-P	fasting C-peptide
FC-P/G	fasting C-peptide to glucose ratio
FPG	fasting plasma glucose
FINS	fasting insulin
IFG	impaired fasting glucose
INS	insulin
ISI-Matsuda	Matsuda index
LDH	lactate dehydrogenase
MTT	3-(4,5-dimethyl-2-thiazolyl)-2,5-diphenyl-2-H-tetrazolium bromide
2hPG	2h post-meal glucose
Rictor	rapamycin-insensitive companion of mTOR
PI3K	phosphoinositide 3-kinase
SVCs	stromal-vascular cells
TBP	TATA-Box Binding Protein
TC	total cholesterol
TG	triglycerides
TMB	tetramethylbenzidine
UA	uric acid
WC	waist circumference

proliferation. Meanwhile, recent studies showed that there were also potential negative regulators that limited the adaptive proliferation of  $\beta$ -cells, leading to an inadequate expansion of  $\beta$ -cell mass. The inadequate compensation of  $\beta$ -cells would result in further increased glucose levels which may trigger the loss of  $\beta$ -cell mass. Thus, much is still unknown about the physiological regulation of  $\beta$ -cell mass in the status of nondiabetic obesity, especially in humans. Understanding the regulatory mechanisms during this adaptive process will shed light on new therapeutic targets for T2DM prevention and treatment.

Recently, multiple studies have shown a novel exosome-like vesicles (ELVs)-mediated mechanism for regulating  $\beta$ -cell mass. ELVs, the smallest class of extracellular vesicles released by cells and taken up by neighboring or distant cells,<sup>5</sup> carry bioactive proteins, lipids, and nucleic acids, functioning in cellular crosstalk.<sup>6</sup> Jalabert et al showed that ELVs released from lipid-induced insulin-resistant muscles increased  $\beta$ -cell proliferation through downregulating the gene expression of Ptch1 in mice.<sup>7</sup> Another research found that miR-106b-5p and miR-222-3p contained in mouse serum ELVs contributed to bone marrow transplantation-induced  $\beta$ -cell regeneration by increasing the proliferation of residual  $\beta$ -cells.<sup>8</sup> Moreover, ELVs released by mouse  $\beta$ -cells under proinflammatory conditions triggered apoptosis of recipient  $\beta$ -cells.<sup>9</sup>

In this study, we aim to investigate whether the ELVs in circulation of humans with nondiabetic obesity play roles in the regulation of  $\beta$ -cell mass, and to further determine whether the protein cargos of ELVs are modulated by obesity and associated with the phenotype of the recipient  $\beta$ -cells.

## Introduction

It has been well recognized that obesity is a significant risk factor for developing type 2 diabetes mellitus (T2DM). A majority of individuals suffering from T2DM are obese.<sup>1</sup> The natural history of the progression of obesity to T2DM remains not fully understood. One crucial contributor is the progressive decline in islet  $\beta$ -cell mass.<sup>2</sup> However, numerous studies have demonstrated that  $\beta$ -cell mass expands adaptively in obesity to compensate for insulin resistance. Several factors in blood circulation including the overload of nutrients, insulin, growth factors, and incretin hormones,<sup>3</sup> as well as the hepatocyte-secreted protein SerpinB1,<sup>4</sup> have been shown to promote  $\beta$ -cell mass expansion mainly through increasing cellular

## Materials and methods

### Subjects

Between June 2017 and July 2019, 81 subjects with simple obesity who visited the Obesity Clinic in our hospital were recruited. Another 102 healthy volunteers with normal weight and matched for age and sex, were recruited as the control group. BMI  $\geq 28$  kg/m<sup>2</sup> is referred to as obesity, and 18.5 kg/m<sup>2</sup>  $\leq$  BMI  $< 24$  kg/m<sup>2</sup> is referred to as normal weight.<sup>10</sup> All subjects (i) were between 18 and 60 years of age, (ii) did not use any medication within the past 3 months, (iii) had no tobacco and alcohol addiction, and (iv) had menstrual regularity in women. Exclusion criteria were subjects who (i) had a fasting blood glucose

level  $\geq 7.0$  mmol/L and 2h glucose level  $\geq 11.1$  mmol/L following an OGTT test, (ii) had moderate or severe hypertension; (iii) had moderate or severe renal and hepatic dysfunctions. All subjects provided written informed consent and the study protocol had the approval of the local Ethical Committee of the First Affiliated Hospital of Chongqing Medical University. The clinical and biochemical parameters were measured as described before.<sup>11,12</sup> The amount of body fat mass and waist circumference (WC) were estimated using a dual-energy X-ray absorptiometry scanner (Lunar DPX-NT; General Electric Healthcare, Little Chalfont, Buckinghamshire, UK, software version 4.7).

Insulin resistance and  $\beta$ -cell secretory function were calculated using the following formulas: HOMA-IR = fasting insulin  $\times$  fasting glucose/22.5; Insulin sensitivity index (ISI-Matsuda) =  $10,000/\sqrt{(\text{fasting glucose} \times \text{fasting insulin}) \times (\text{OGTT mean glucose} \times \text{OGTT mean insulin})}$ ; Fasting C-peptide to Glucose Ratio (FC-P/G) = fasting C-peptide/fasting glucose; Insulin secretion index ( $\text{AUC}_{\text{INS/G}}$ ) = AUC of insulin/AUC of glucose.

### Isolation and identification of ELVs

Blood sample (4 ml) of each subject was obtained after an overnight fast. For ELV isolation, the plasma samples were centrifuged two times to remove debris (2000 $\times$ g at 4 °C for 30 min and 12,000 $\times$ g at 4 °C for 45 min). Then the supernatants were ultra-centrifuged (Beckman Optima XPN-100, USA) at 110,000 $\times$ g at 4 °C for 2 h to obtain ELV pellets which were resuspended in PBS and passed through a 0.22  $\mu\text{m}$  filter. Afterward, the ELV pellets were washed two times by ultra-centrifuging at 110,000 $\times$ g at 4 °C for 70 min. Finally, ELV pellets were resuspended in 50–200  $\mu\text{L}$  sterile PBS.

ELV markers were detected by Western blotting. The morphology and size distribution of ELVs were identified by transmission electron microscopy (TEM, Hitachi7500, HITACHI, Japan) and nano-sight tracking analysis (NTA) (ZetaView PMX 110, Particle Metrix, Meerbusch, Germany).

### Culture of isolated islets and Min6 cells

Primary mouse islets were isolated from 10-wk old male C57BL/6 mice (Experimental Animal Center of Chongqing Medical University, Chongqing, China) fed with a regular diet. Mouse pancreas was cannulated with 2 ml cold Krebs-BSA2% buffer (KRBB) containing collagenase P (1.3 mg/2 ml) (Roche Diagnostics, Shanghai, China) and then removed, followed by incubation in a water bath at 37 °C for 15 min. After digestion, the pancreas pellets were washed three times in cold KRBB. Single islets were manually selected under a microscope. Isolated islets and Min6 cells (BeNa Culture Collection, Beijing, China, [www.bnbio.com/](http://www.bnbio.com/)) were cultured in PR1640 medium containing 10% exosome-depleted FBS (BI, Shanghai, China) and 1% Penicillin/Streptomycin (Beyotime Institute of Biotechnology, Shanghai, China) at 37 °C with 5%  $\text{CO}_2$ . In some experiments, Min6 cells and islets were cultured in serum-free medium.

### Culture of adipose tissue explants, adipocytes and stromal-vascular cells (SVCs)

Human omental adipose tissues (AT) were obtained from 10 subjects with normal weight (BMI:  $21.3 \pm 2.0$  kg/m<sup>2</sup>) and 8 subjects with simple obesity (BMI:  $31.6 \pm 7.4$  kg/m<sup>2</sup>) undergoing laparoscopic cholecystectomy (see Table S2 for more characteristics). Mouse epididymal AT were from 14-wk-old C57BL/6 mice fed with a regular diet or a high-fat diet (60% fat, Research Diets, Inc., New Brunswick, USA) for 10 weeks. For explant culture, AT were finely minced and 40 pieces per well were incubated in 5 ml MEM supplemented with 0.5% BSA, 50  $\mu\text{M}$  ascorbic acid (Sigma–Aldrich, Shanghai, China), and 1% Penicillin/Streptomycin for 24 h.<sup>13</sup> Lactate dehydrogenase (LDH) release test (kit from Beyotime Institute of Biotechnology) was performed to evaluate the viability of explants during 24 h culture (Fig. S4A).<sup>14</sup> For adipocytes and SVC culture, minced AT was digested and separated into adipocytes and SVC fractions as described before.<sup>15</sup> Isolated cells were then cultured in 5 ml MEM with 10% ELV-depleted FBS and 1% Penicillin/Streptomycin for 24 h. In some experiments, cultured human omental AT explants were treated with or without human insulin (Novo Nordisk, Copenhagen, Denmark) for 24 h. The culture medium (20–30 mL) was collected for ELV isolation as described above.

### Uptake of ELVs by Min6 cells and primary islets

ELVs were labeled with fluorescent dye PKH67 (Sigma–Aldrich, Shanghai, China) and then added into the culture medium of Min6 cells or primary islets. After 12 h of culture, the Min6 cells or islets were observed under a fluorescence microscope (Olympus IX5, Japan).

### MTT assay

Min6 cells were incubated with human ELVs for 48 h. Then, 5 mg/ml MTT (Sangon Biotech, Shanghai, China) was added and incubated for another 4h. Optical density (OD) values were read at 490 nm.

### Proliferation assays

Min6 cell proliferation was detected by two EdU methods (with TMB coloration and fluorescent dye), and the primary islet proliferation was detected by EdU with fluorescent dye. Briefly, Min6 cells were incubated with ELVs for overnight, and 10 $\mu\text{M}$  EdU was added 2 h before cells were fixed. Islets were seeded onto Matrigel (#356230, Corning, NY, US) coated coverslips to help the adherence and growth of islets, and incubated with ELVs and 10  $\mu\text{M}$  EdU for 48 h. EdU was detected using EdU Cell Proliferation Kit with TMB (Beyotime Institute of Biotechnology) or EdU AlexaFluor555 Imaging Kit (Invitrogen, CA, US). In the latter assay, cells and islets were counterstained with anti-insulin antibody (#ab181547, Abcam, Shanghai, China) and fluorescent secondary antibody (#4412, Cell Signaling Technology, Shanghai, China) to define  $\beta$ -cells and islets.

## Apoptosis assays

Min6 cells were seeded in a 24-well plate and cultured with human ELVs for 48 h. Then, cells were collected and double-stained with fluorescein isothiocyanate (FITC)-Annexin V and propidium iodide (PI). The apoptosis rates of cells were detected using Flow Cytometer (FACS, BD Bioscience, San Jose, CA) and analyzed using CellQuest software (BD Biosciences).

## Glucose-stimulated insulin secretion (GSIS) assays

Ten size-matched islets per well were incubated with 20  $\mu\text{g}/\text{mL}$  ELVs for 48 h. Islets were then starved at 37  $^{\circ}\text{C}$  for 1 h in Krebs-BSA0.1% (KRBB) without glucose and subsequently incubated at 37  $^{\circ}\text{C}$  for 1 h in KRBB supplemented with 3 mM or 25 mM glucose. The supernatants were subjected to mouse insulin ELISA Kit (Raybiotech Inc., Parkway Lane, USA).

## Quantitative proteomic analysis by tandem mass tag (TMT) technology

The experiments were performed by Shanghai Applied Protein Technology Co., Ltd. (Shanghai, China). Proteins of ELVs were extracted by SDT lysis buffer [4%(w/v) SDS, 100 mM Tris/HCl pH7.6, 0.1M DTT]. A total of 200  $\mu\text{g}$  proteins for each sample was digested by the Filter aided proteome preparation. Then, 100  $\mu\text{g}$  peptide mixture of each sample was labeled using TMT reagent (Thermo Fisher Scientific, MA, USA). The TMT-labeled digested samples were fractionated by a Pierce high pH reversed-phase fractionation kit (Thermo Fisher Scientific) and subsequently separated by HPLC system (Easy nLC) (Thermo Fisher Scientific Proxeon Biosystems). A mass spectrometry analysis was performed on a Q Exactive mass spectrometer (Thermo Fisher Scientific) to acquire the MS data. Proteins were identified and quantified by filtering the MS/MS spectra via a MASCOT engine (Matrix Research; version 2.2), which was embedded in Proteome Discoverer 1.4 (Thermo Fisher Scientific).

## ELISA

The Omentin-1 levels in ELVs were quantified by an ELISA Kit (Cusabio, Shanghai, China). The total and the phosphorylated Rictor levels in ELVs were semi-quantified by ELISA (Raybiotech) as the protein levels were presented as OD values. ELV proteins were extracted by PBS with 1% Triton-X100 and measured by BCA Protein AssayKit (Beyotime Institute of Biotechnology). Exosomal levels of Rictor and Omentin-1 were normalized to total ELV protein levels in each sample.

## Real-time quantitative polymerase chain reaction (RT-qPCR)

Total RNA from Min6 cells or islets was extracted by using TRIzol (Invitrogen). RT-qPCR was performed with designed primers (Table S1), as described earlier.<sup>16</sup> 18srRNA were

used as reporter genes. Relative changes in the expression level of one specific gene were presented as  $2^{-\Delta\Delta\text{Ct}}$ .

## Western blot

Since there is still no standard loading control for ELVs and the widely used loading controls (e.g.,  $\beta$ -actin and tubulin) were absent or very weak in some of our ELV protein samples, the loading controls were not served for ELVs.<sup>17,18</sup> An exact of 20  $\mu\text{g}$  ELV proteins were dissolved in Laemmli buffer, subjected to SDS-PAGE under reducing and heat-denaturing conditions and then transferred to the PVDF membrane. The antibodies (see Table S2 for details) were used for immunodetection. Signals were revealed by enhanced chemiluminescence (Amersham Imager 600, GE, USA).

## Overexpression of Omentin-1 in 3T3-L1 preadipocytes and Min6 cells

3T3-L1 preadipocytes were cultured in DMEM with 10% ELV-depleted Calf serum (Sigma–Aldrich) (centrifuged at 120,000 $\times$ g at 4  $^{\circ}\text{C}$  for 15 h to deplete ELVs) and transfected with a plasmid pReceiver-M02 containing the mouse Omentin-1 sequence or a control plasmid containing a scrambled sequence (GeneCopoeia, Guangzhou, China) using Lipofectamine 3000 Transfection Reagent (Invitrogen). After 48 h culture, the medium was collected for ELVs isolation. In some experiments, Min6 cells were transfected with the same plasmids and cultured in PR1640 medium with or without FBS.

## Statistical analysis

Statistical analysis was performed using SPSS Statistics (IBM, Armonk, NY, version 20). Variables were presented as means  $\pm$  SD or SEM. Means of continuous variables were compared using the unpaired *t*-test or Mann–Whitney test. The percentage differences between groups were compared using  $\chi^2$  tests. Correlations of Rictor and Omentin-1 with the clinical variables were evaluated by Pearson or Spearman analysis. Their independent associations were evaluated by multiple stepwise regression analysis. The differences and associations were considered statistically significant at  $P < 0.05$ .

## Results

### Clinical and biochemical characteristics of subjects

As shown in Table 1, subjects with simple obesity had obvious more fat accumulations (greater WC, subcutaneous fat mass, and visceral fat mass) and a worse metabolic profile (higher BP, glucose, UA, ALT, AST, TG, and lower HDL), when compared to subjects with normal weight. Moreover, subjects with simple obesity had significantly increased insulin secretion (FINS, FC-P/G,  $\text{AUC}_{\text{INS/G}}$ ), and insulin resistance (higher HOMA-IR, lower ISI-matsuda).

### Circulating ELVs isolated from subjects with simple obesity impaired mouse islet $\beta$ -cell proliferation without affecting its apoptosis, secretion, and inflammation

Firstly, ELVs were isolated from plasma of the two groups by ultra-centrifuge. Isolated ELVs were characterized according to the International Society of Extracellular Vesicles guidelines.<sup>19</sup> Electron microscopy showed the cup-shaped morphology (Fig. 1A). Similar size distribution was confirmed by NTA in two groups with an average diameter of around 110 nm (Fig. 1B). By Western blot, proteins of ELV extracts were further confirmed to be enriched with ELV markers (CD9, CD63, and TGS101) (Fig. 1C). Moreover, these ELVs were identified to be efficiently taken up by Min6 cells and islets (Fig. 2A, B).

We treated Min6 cells with different concentrations (5  $\mu$ g/mL, 10  $\mu$ g/mL, 20  $\mu$ g/mL) of ELVs (Fig. S1), and found that 20  $\mu$ g/mL ELVs from subjects with simple obesity (O-

ELVs) significantly inhibited viability (Fig. 3A) and proliferation (Fig. 3B, C) of Min6 cells comparing with the ELVs from subjects with normal weight (N-ELVs). This inhibitory effect of O-ELVs was further proved in primary mouse islets by EdU incorporation (Fig. 3D). It should be noted that we took human ELVs to treat mouse  $\beta$ -cells and islets. This is due to the findings that ELVs can be taken up by cells with a low possibility of immune rejection.<sup>20</sup> In fact, by using PBS and BSA as controls, 20  $\mu$ g/mL human ELVs were shown not to cause injury in mouse  $\beta$ -cells and islets.

Nevertheless,  $\beta$ -cell apoptosis and insulin secretory function was not affected by O-ELVs (Fig. 4A, B). Moreover, given obesity is a low-grade pro-inflammatory state, we examined whether the circulating ELVs transmitted inflammatory signals, which is also crucial for  $\beta$ -cell growth. Likewise, there were no differences in the NF- $\kappa$ B activity (Fig. 4C) and the gene expression of I $\kappa$ B- $\alpha$  (an endogenous inhibitor of NF- $\kappa$ B activity), as well as the gene expression of pro-inflammatory cytokines (TNF- $\alpha$ , and CCL2)<sup>21</sup> between Min6 cells treated with O-ELVs and N-ELVs (Fig. 4D).

**Table 1** Data are means  $\pm$  SD or median (interquartile ranges) or number (percentage) for 102 subjects with normal weight (Normal weight) and 81 subjects with simple obesity (Obesity).

	Normal weight ( <i>n</i> = 102)	Obesity ( <i>n</i> = 81)	<i>P</i> value
Age (years)	32.98 $\pm$ 6.68	31.30 $\pm$ 9.95	0.19
Male, <i>n</i> (%)	50 (49.02%)	39 (48.14%)	0.97
SBP (mmHg)	113.19 $\pm$ 14.51	130.20 $\pm$ 14.33	<0.01
DBP (mmHg)	69.92 $\pm$ 9.48	80.31 $\pm$ 9.19	<0.01
FPG (mmol/L)	5.25 $\pm$ 0.55	5.60 $\pm$ 0.72	<0.01
2hPG (mmol/L)	7.13 $\pm$ 1.59	8.54 $\pm$ 2.51	<0.01
TC (mmol/L)	4.47 $\pm$ 0.81	4.30 $\pm$ 0.66	0.18
TG (mmol/L)	1.17 $\pm$ 0.72	1.83 $\pm$ 1.14	<0.01
HDL (mmol/L)	1.48 $\pm$ 0.37	1.09 $\pm$ 0.28	<0.01
LDL (mmol/L)	2.73 $\pm$ 0.73	2.78 $\pm$ 0.65	0.64
Cr ( $\mu$ mol/L)	70.08 $\pm$ 16.38	67.49 $\pm$ 14.62	0.24
UA ( $\mu$ mol/L)	323.71 $\pm$ 83.04	449.86 $\pm$ 104.25	<0.01
ALT (IU/L)	14.5 (11.00–22.00)	37.5(23.75–60.25)	<0.01
AST (IU/L)	17.00 (14.00–21.00)	23.5 (18.75–35.50)	<0.01
<b>Indices of Obesity</b>			
BMI (kg/m <sup>2</sup> )	21.11 $\pm$ 1.82	33.42 $\pm$ 4.33	<0.01
WC (cm)	82.25 $\pm$ 5.51	111.57 $\pm$ 10.81	<0.01
VAT mass (g)	265.39 $\pm$ 100.05	626.52 $\pm$ 243.77	<0.01
SAT mass (g)	716.13 $\pm$ 301.04	1707.82 $\pm$ 479.65	<0.01
<b>Indices of insulin resistance and secretion</b>			
HOMA-IR	1.18 $\pm$ 0.78	3.97 $\pm$ 2.71	<0.01
ISI-matsuda	171.54 $\pm$ 83.92	57.16 $\pm$ 38.90	<0.01
FINS (uU/ml)	4.87 $\pm$ 3.00	15.33 $\pm$ 9.45	<0.01
AUC <sub>INS/G</sub>	4.32 $\pm$ 1.98	10.94 $\pm$ 5.84	<0.01
FC-P/G	0.33 $\pm$ 0.08	0.77 $\pm$ 0.33	<0.01

*P* values for comparisons between two groups are based on unpaired *t*-test or Mann–Whitney test (when the data are not normally distributed) or  $\chi^2$  test.

Abbreviations: SBP = systolic blood pressure; DBP = diastolic blood pressure; BMI = body mass index; WC = waist circumference; FPG = fasting plasma glucose; 2hPG = 2h post-meal glucose; TC = total cholesterol; TG = triglycerides; FINS = fasting insulin; Cr = creatinine; UA = uric acids; ALT = alanine aminotransferase; AST = aspartate aminotransferase; VAT = visceral fat; SAT = subcutaneous fat. FC-P/G = fasting C-peptide to Glucose Ratio; ISI-Matsuda = Matsuda index; AUC<sub>INS/G</sub> = Insulin secretion index.

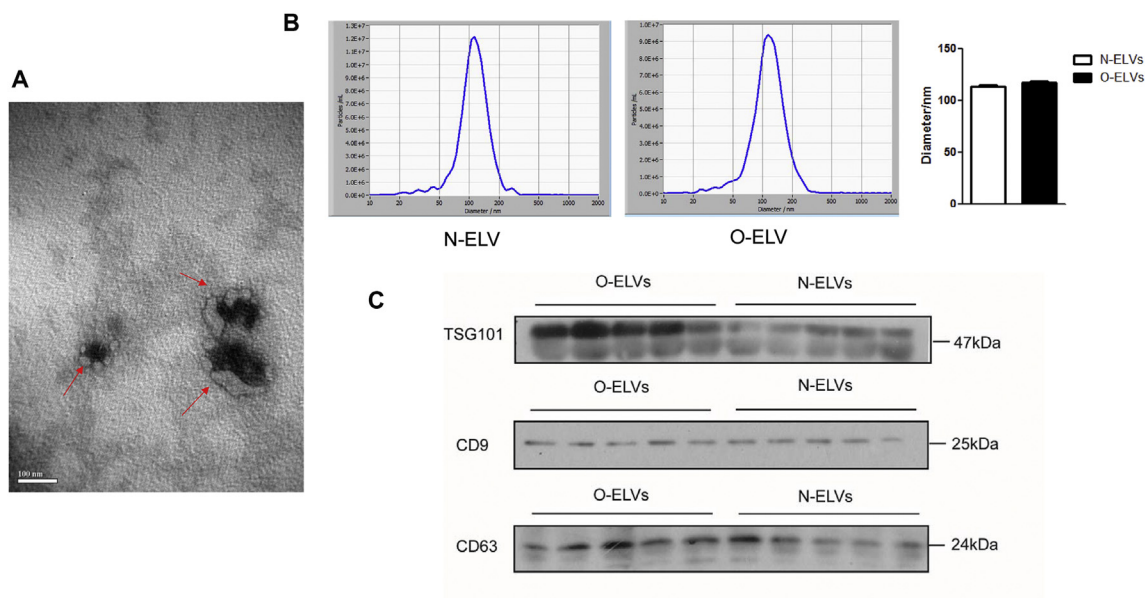


**Figure 1** Identification of ELVs isolated from human plasma. (A) Transmission electron microscopy exhibits the cup-shaped morphology of ELVs. Bar indicates 100 nm. (B) Nano-sight tracking analysis (NTA) shows the size distribution of ELVs. Data are presented as average diameters (nm). Results are means  $\pm$  SEM for 4 samples per group. (C) Western blot confirmed the presence of ELV specific markers (CD9, CD63, and TSG101). N-ELVs: ELVs isolated from subjects with normal weight; O-ELVs: ELVs isolated from subjects with simple obesity.

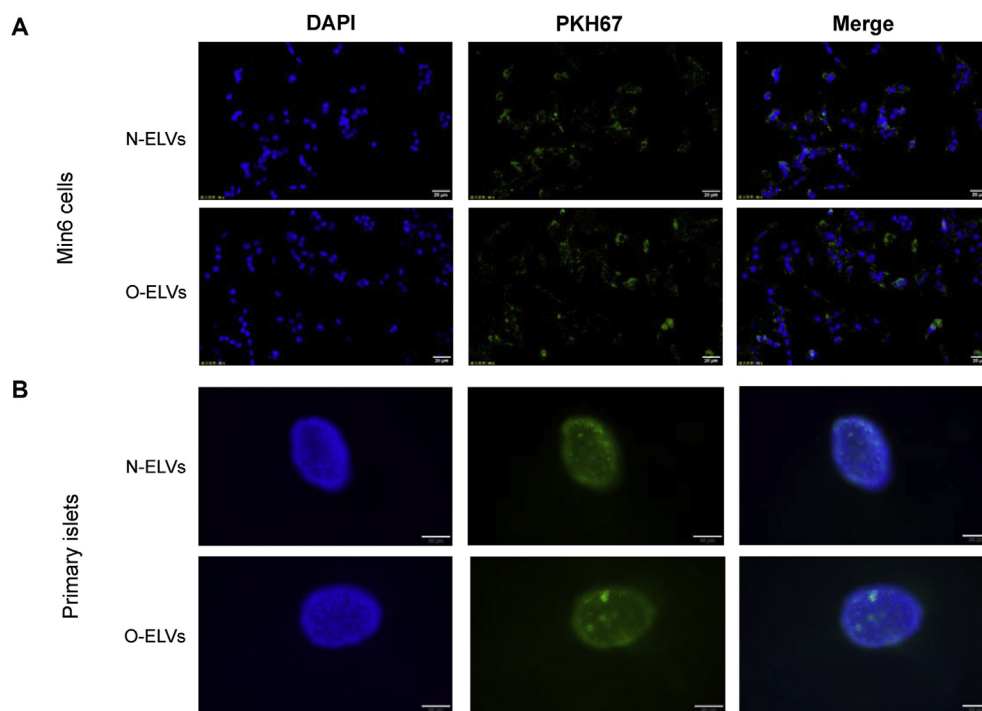


**Figure 2** Uptake of ELVs by Min6 cells and primary islets. ELVs were labeled with fluorescent dye PKH67 (green). (A) Representative images (40x magnification) of labeled ELVs in Min6 cells. (B) Representative images (20x magnification) of labeled ELVs in primary islets. Cells and islets were co-stained with DAPI to identify nuclei (blue). N-ELVs: ELVs isolated from plasma of subjects with normal weight; O-ELVs: ELVs isolated from plasma of subjects with simple obesity.

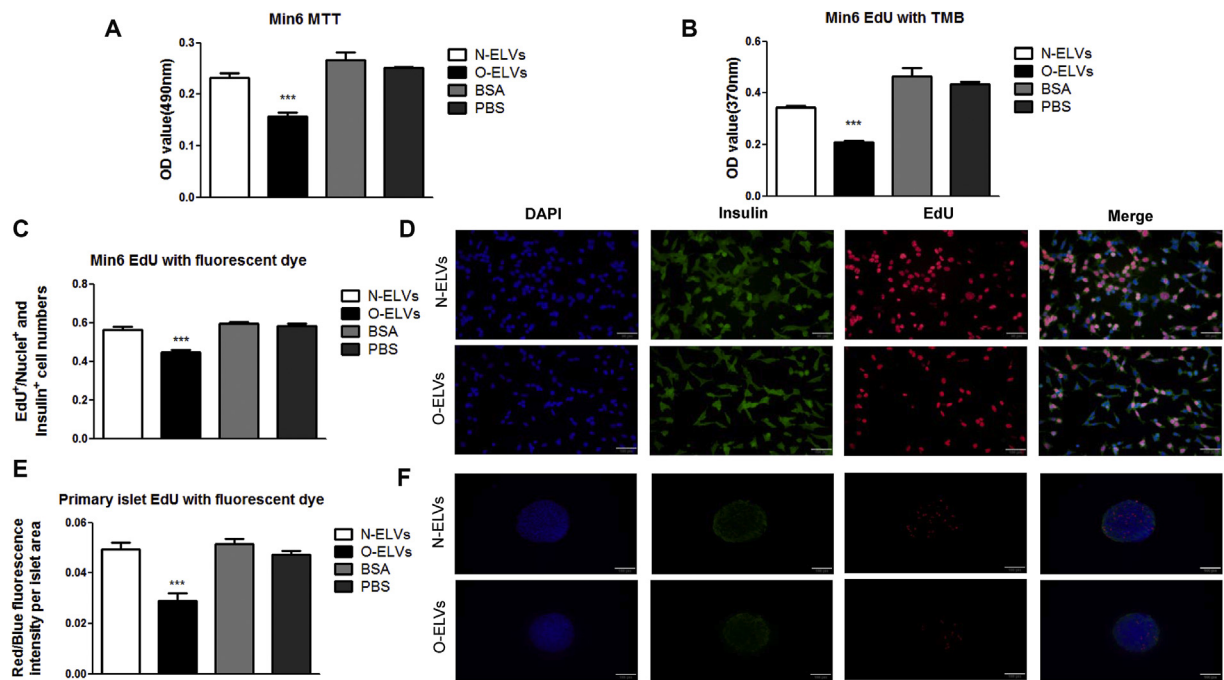


**Figure 3** Effect of circulating ELVs of subjects with simple obesity on  $\beta$ -cell viability and proliferation. (A) Min6 cells (300 cells/well) were treated with 200  $\mu$ g/mL ELVs for 48 h and incubated with 5 mg/ml MTT for 4 h. Results are means  $\pm$  SEM for 4 repeated experiments. (B) Min6 cells (3000 cells/well) were treated with 200  $\mu$ g/ml ELVs for overnight and incubated with EdU for 2 h. EdU was detected by TMB coloration. (C) Min6 cells ( $2 \times 10^5$  cells/well) were treated as in (B) and EdU was detected by fluorescent dye. Data were presented as a ratio (EdU<sup>+</sup> cell numbers/Nuclei<sup>+</sup> and Insulin<sup>+</sup> cell numbers). (D) Representative images (40x magnification) of Min6 cells labeled with EdU (red), nuclei (blue), and insulin (green). (E) Primary islets were treated with 200  $\mu$ g/mL ELVs and EdU for 48 h. EdU was detected by fluorescent dye. Data were presented as a ratio (Red fluorescence intensity/Blue fluorescence intensity per islet area). (F) Representative images (20x magnification) of the islets labeled with EdU (red), nuclei (blue), and insulin (green). Results shown herein (B, C, E) are the means  $\pm$  SEM for 3 repeated experiments. N-ELVs: ELVs isolated from plasma of subjects with normal weight; O-ELVs: ELVs isolated from plasma of subjects with simple obesity. \*\*\* $P < 0.001$  vs. N-ELVs.

### Circulating ELVs from subjects with simple obesity carried altered protein cargos

To investigate the mechanisms underlying the ELV-mediated regulation of  $\beta$ -cell proliferation, we analyzed the proteomics of plasma ELVs isolated from the two groups. Owing to TMT technology, a total of 529 proteins were detectable in ELVs of both groups (Fig. S2). Among them, the abundance of 11 proteins was increased, while 18 was decreased (Fold Change  $> 1.2$ ,  $P < 0.05$ ) (Table 2). The roles of these proteins were further annotated by GO and KEGG signaling pathways. The most significantly annotated pathway was the mTOR signaling pathway and one protein enriched for this pathway was the Rapamycin-insensitive companion of mTOR (Rictor) which was reduced by 65% in O-ELVs (Table 2). mTOR signaling pathway has long been known to regulate cell growth and proliferation in response to insulin, nutrients, and growth factors.<sup>22</sup> Another protein that had established roles in proliferation<sup>23</sup> was the Intelectin-1 (also named Omentin-1) which was reduced by 27% in O-ELVs (Table 2). The presence of Rictor and Omentin-1 in ELVs was further verified by Western blot (Fig. 5A, B). Notably, both the total and phosphorylated Rictor were present in ELVs (Fig. 5A).

According to the big heterogeneities among human plasma samples, the protein abundance of Omentin-1, as well as the total and phosphorylated Rictor, were quantified by ELISA in a larger sample. In agreement with the result of proteomics, the levels of both forms of Rictor decreased by 25% and 23% respectively in O-ELVs (Fig. 5C), and the levels of Omentin-1 decreased by 51% (Fig. 5D).

### The circulating ELV-carried Rictor and Omentin-1 were associated with obesity-linked pathologic conditions

To get insight into whether the dysregulation of these two exosomal proteins was associated with obesity-linked pathologic conditions, we analyzed their relationships with the clinical variables. The exosomal phosphorylated Rictor negatively correlated with the FC-P/G (a more accurate index reflecting endogenous insulin secretion)<sup>24</sup> and TG. The exosomal Omentin-1 negatively correlated with insulin levels (FINS, FC-P/G, and AUC<sub>INS/G</sub>) and HOMA-IR, while positively correlated with the ISI-matsuda and HDL. Moreover, both the exosomal phosphorylated Rictor and Omentin-1 showed negative correlations with abdominal

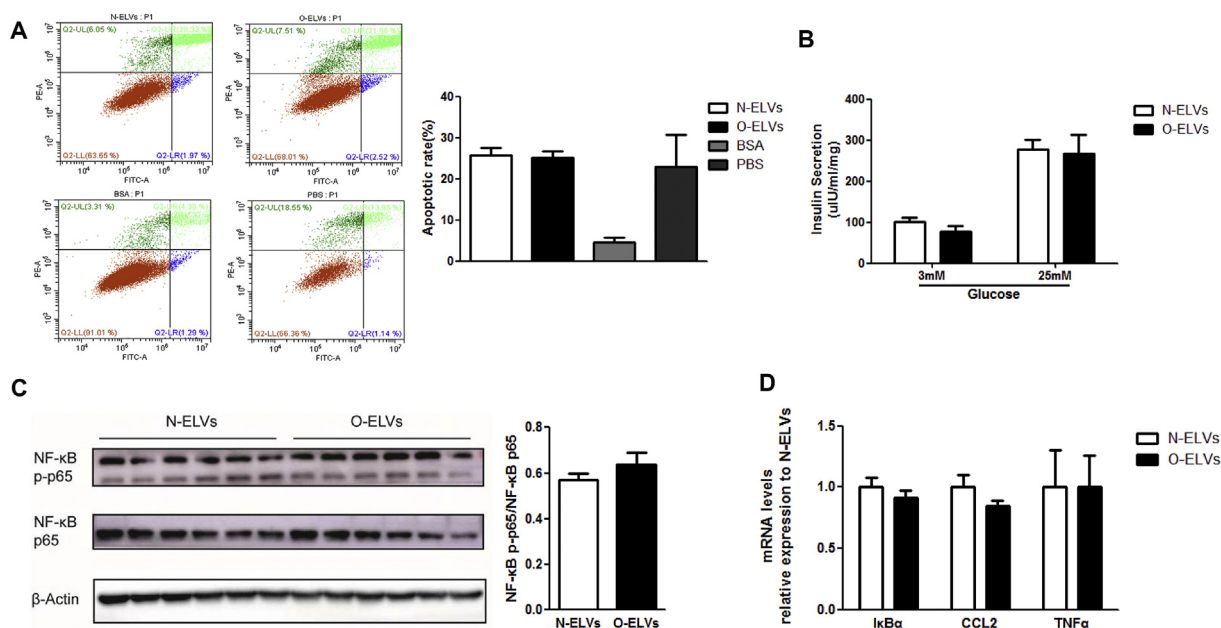


**Figure 4** Effects of circulating ELVs of subjects with simple obesity on  $\beta$ -cell apoptosis, secretion, and inflammation. **(A)** Min6 cells were treated with 200  $\mu\text{g}/\text{mL}$  ELVs for 48 h. Data are presented as the apoptosis rate (apoptotic cell numbers/total cell numbers). **(B)** Primary islets were treated with 200  $\mu\text{g}/\text{mL}$  ELVs for 48 h, the basal and the glucose-stimulated insulin levels were measured by ELISA. Insulin secretion levels were normalized to total islet protein levels. **(C)** Min6 cells were treated with 200  $\mu\text{g}/\text{mL}$  ELVs for 60 min, NF- $\kappa$ B activity (pp65) were measured by Western blot and normalized to p65. A representative blot is shown on the left. **(D)** Min6 cells were treated with 200  $\mu\text{g}/\text{mL}$  ELVs for 48 h. Gene expression of IkB- $\alpha$ , TNF- $\alpha$  and C-C motif ligand 2 (CCL-2) was quantified by RT-qPCR and presented as relative expression compared to the values of N-ELVs. Results shown herein (A–D) are the means  $\pm$  SEM for 3 repeated experiments. N-ELVs: ELVs isolated from subjects with normal weight; O-ELVs: ELVs isolated from subjects with simple obesity.

obesity (BMI, WC, and visceral fat mass) (Table 3). By multivariate analysis, the exosomal phosphorylated Rictor was independently associated with the TG ( $\beta = -0.36$ ,  $P = 0.04$ ), while the Omentin-1 was mainly related to the index of insulin resistance (ISI-matsuda) ( $\beta = 0.52$ ,  $P < 0.01$ ).

### The ELV-carried Omentin-1 promoted $\beta$ -cell proliferation *in vitro*

To validate whether the ELV-carried proteins affect  $\beta$ -cell proliferation, we tried to modify the specific protein expressions in ELVs. First, we determined the cell source of the two exosomal proteins. Since above data showed that circulating exosomal Rictor and Omentin-1 were correlated with visceral fat mass, we investigated the ELVs released from the visceral AT (Fig. S3). However, Rictor was not detectable in AT-released ELVs of both humans and mice (data not shown). Expectedly, Omentin-1 was present in ELVs released by human omental and mouse epididymal AT. Compared to the human lean omental AT-released ELVs, Omentin-1 protein levels in the obese omental AT-released ELVs were decreased (Fig. S4B). Unlike humans, Omentin-1 was not changed in obese mouse epididymal AT-released ELVs (Fig. S4D). This discrepancy may result from the fact that mouse Omentin-1 was highly secreted by the intestine, but not visceral AT.<sup>22</sup> Furthermore, we found that Omentin-

1 was mainly present in adipocyte-released ELVs compared to SVC-released ELVs (almost undetectable) in both humans (Fig. S4C) and mice (Fig. S4E), although the mRNA expression of Omentin-1 is much lower in adipocytes than in SVCs.<sup>22</sup>

Therefore, we focused on ELV-carried Omentin-1 and next investigated its role in  $\beta$ -cell proliferation. We utilized 3T3-L1 preadipocytes overexpressing Omentin-1 (Fig. 6A) to produce Omentin-1-overexpressed ELVs (Fig. 6B). Compared to control ELVs, the Omentin-1-overexpressed ELVs promoted  $\beta$ -cell (Fig. 6C–E) and islet proliferation (Fig. 6F, G).

### The ELV-carried Omentin-1 activated Akt and increased cyclin D2 in $\beta$ -cells

To understand possible mechanisms by which ELV-carried Omentin-1 potentiates proliferation, we investigated whether it modulated the activation of Akt, a key kinase in cellular proliferation<sup>23</sup>. Indeed, Omentin-1-overexpressed ELVs enhanced the Akt phosphorylation at both 15 and 60 min in min6 cells, compared to control ELVs (Fig. 7A, B). Also, the cell cycle stimulator, Cyclin D2,<sup>25,26</sup> was upregulated by Omentin-1-overexpressed ELVs (Fig. 7C).

To further evaluate whether Omentin-1 was a key component in the role of circulating ELVs on  $\beta$ -cell



**Table 2** The protein components contained in ELVs were identified and quantified by Quantitative Proteomic Analysis based on Tandem mass tag (TMT) technology.

Accession	Protein name	Average Obese/Normal	P value
P02743	Serum amyloid P-component (APCS)	1.23	0.001
P02656	Apolipoprotein C-III(APOC3)	1.28	0.010
V9GYE7	Complement factor H-related protein 2(CFHR2)	1.30	0.013
B4DVE1	cDNA FLJ53478, highly similar to Galectin-3-binding protein	1.22	0.016
P02741	C-reactive protein (CRP)	1.86	0.017
A0N7I9	F5-20 (Fragment)	1.73	0.025
B1AKG0	Complement factor H-related protein 1(CFHR1)	1.20	0.028
G3XAM2	Complement factor I(CFI)	1.45	0.031
K7ER74	APOC4-APOC2 readthrough (NMD candidate)	1.37	0.032
A0A0G2JRQ6	Uncharacterized protein (Fragment)	1.51	0.035
P01024	Complement C3	1.21	0.040
F8WBH5	Proteasome activator complex subunit 4(PSME4)	0.19	0.000
A0A0G2JMI3	Immunoglobulin heavy variable 1-69-2(IGHV1-69-2)	0.14	0.001
Q6MZG5	Putative uncharacterized protein DKFZp686D06190	0.41	0.002
G3XAP6	Cartilage oligomeric matrix protein (COMP)	0.80	0.003
H0YFX9	Histone H2A (Fragment)	0.77	0.005
B5MEF5	Sushi, nidogen and EGF-like domain-containing protein 1 (SNED1)	0.32	0.005
B4E1B2	cDNA FLJ53691, highly similar to Serotransferrin	0.68	0.005
Q6R327	<b>Rapamycin-insensitive companion of mTOR (RICTOR)</b>	0.35	0.007
A2IPI3	HRV Fab N28-VL (Fragment)	0.57	0.008
A0A075B7D0	Immunoglobulin heavy variable 1/OR15-1 (non-functional) (Fragment) (IGHV1OR15-1)	0.67	0.009
P43251	Biotinidase	0.77	0.010
L8E853	von Willebrand factor (VWF)	0.74	0.010
Q5NV91	V2-19 protein (Fragment)	0.46	0.017
Q5IWS5	<b>Intelectin 1 (ITLN1)</b>	0.73	0.026
Q9H9V0	cDNA FLJ12531 fis, clone NT2RM4000199	0.52	0.027
Q5NV83	V3-3 protein (Fragment)	0.70	0.029
Q9BTS4	phosphatidylinositol-4,5-bisphosphate 3-kinase catalytic subunit alpha/beta/delta (PIK3CA_B_D)	0.82	0.036
A0A0C4DH39	Immunoglobulin heavy variable 1-58(IGHV1-58)	0.61	0.046

Results are presented as the average ratios of the protein levels in ELVs of subjects with simple obesity to the protein levels in ELVs of subjects with normal weight (average Obese/Normal) for 3 mixed samples (9 subjects) per group.

proliferation, the activity of Akt and protein levels of Cyclin D2 were in turn checked in Min6 cells treated by human circulating ELVs. Compared to ELVs of subjects with normal weight, Cyclin D2 were downregulated by the ELVs of subjects with simple obesity (Fig. 7D), while the Akt phosphorylation was not changed possibly due to the complexity of ELV cargos (Fig. S5).

### The presence of Omentin-1 protein *per se* in $\beta$ cells promoted cellular proliferation

Considering the complexity of ELV cargos, we overexpressed Omentin-1 (which is not originally expressed in  $\beta$  cells) in the site of Min6 cells (Fig. 8A) to study the direct effect of this protein on  $\beta$ -cell proliferation. This experiment recapitulated the data of ELV-carried Omentin-1. The Min6 cells expressing Omentin-1 exhibited increased cellular proliferation (Fig. 8B), Akt activity (Fig. 8C) and protein levels of Cyclin D2 (Fig. 8D).

### The ELV-carried Omentin-1 was downregulated by insulin *in vitro*

Considering the strong association between Omentin-1 and insulin resistance (hyperinsulinemia), we finally investigated the direct effect of insulin on exosomal Omentin-1. As expected, Omentin-1 protein levels in ELVs released from human omental AT of subjects with normal weight were downregulated by 10 nM, 100 nM, and 1  $\mu$ M of insulin treatment (Fig. 9).

### Discussion

In the present study, we aimed to investigate the role of the circulating ELVs in  $\beta$ -cell mass regulation in the status of nondiabetic obesity. Our results showed for the first time that circulating ELVs of subjects with simple obesity may act as a negative regulator for  $\beta$ -cell mass through inhibiting  $\beta$ -cell proliferation. Consistently, Ji et al demonstrated

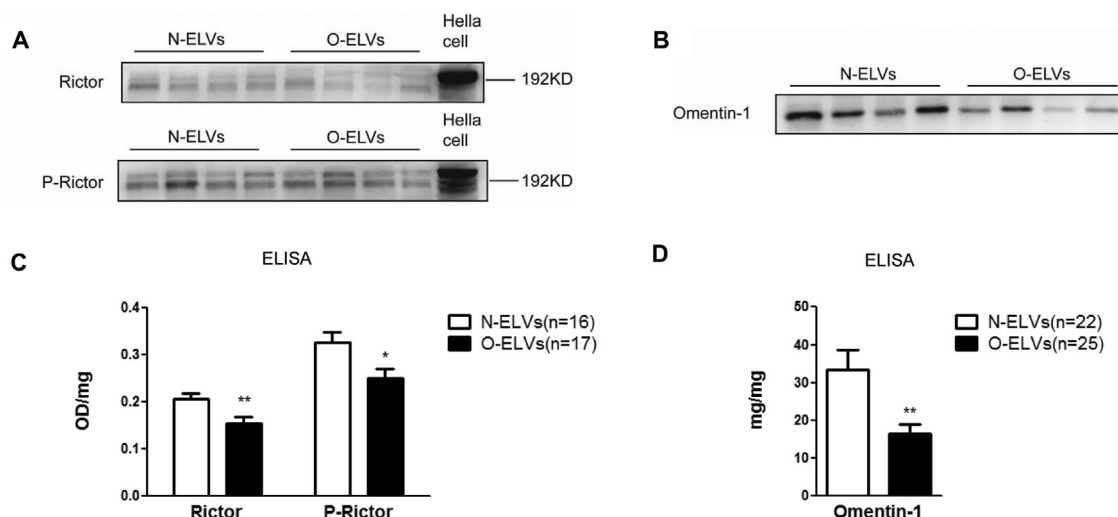


**Figure 5** Verification of the presence and protein abundance of Rictor and Omentin-1 in human circulating ELVs. (A, B) The representative blots show the presence of Rictor and Omentin-1 in human circulating ELVs. (C, D) The protein abundance of Rictor and Omentin-1 in human circulating ELVs was quantified by ELISA and normalized to total ELV protein levels. Results are means  $\pm$  SEM for 16–25 subjects per group. N-ELVs: ELVs isolated from plasma of subjects with normal weight; O-ELVs: ELVs isolated from plasma of subjects with simple obesity. \* $P < 0.05$ , \*\* $P < 0.01$  vs. N-ELVs.

that TLR2 and TLR4 activated in diet-induced obese mice inhibited  $\beta$ -cell proliferation through blocking the nuclear entry of cell cycle regulators, cyclin D2/Cdk4 complex.<sup>27</sup> Also, a prior study by Carboneau et al showed that Prostaglandin E2 Receptor, EP3, restricted  $\beta$ -cell proliferation induced by hyperglycemia and insulin resistance through phospholipase C (PLC)- $\gamma$ 1 activity in mice and humans.<sup>28</sup> Their findings, together with ours, suggested that  $\beta$ -cell proliferation in obesity was regulated by both positive and negative signals. It has been proposed that an ability to increase  $\beta$ -cell mass compensation in obesity is key to preventing T2DM.<sup>3</sup> The existence of negative regulators may, at least in part, explain why some obese individuals

have a failure to initially expand  $\beta$ -cell mass in response to obesity, which predisposes them to the eventual development of T2DM.<sup>3</sup> Thus, targeting the negative regulators to relieve the limitations may also be a promising strategy to increase  $\beta$ -cell mass.

Since the roles of ELVs are played by their carried bioactive cargos, we analyzed the protein components in circulating ELVs isolated from both groups. By proteomic analysis, we found a pattern of proteins in circulating ELVs was altered in the status of nondiabetic obesity. Among them, Rictor and Omentin-1 were identified as decreased in circulating ELVs of people with simple obesity. Rictor, an essential component of the PI3K/mTORC2/AKT signaling

**Table 3** The exosomal protein levels of phosphorylated Rictor and Omentin-1 were detected by ELISA.

	Pho-Rictor/P ( <i>n</i> = 33)		Omentin/P ( <i>n</i> = 47)	
	Correlation Coefficient ( <i>r</i> )	<i>P</i> value	Correlation Coefficient ( <i>r</i> )	<i>P</i> value
FINS	−0.26	0.14	−0.61	< 0.01
HOMA-IR	−0.22	0.22	−0.43	< 0.01
FC-P/G	−0.47	< 0.01	−0.59	< 0.01
ISI-matsuda	0.29	0.10	0.64	< 0.01
AUC <sub>INS/G</sub>	−0.23	0.21	−0.48	< 0.01
TG	−0.42	0.02	−0.32	0.05
HDL	0.29	0.11	0.36	0.03
BMI	−0.40	0.02	−0.56	< 0.01
WC	−0.34	0.05	−0.63	< 0.01
VAT mass	−0.40	0.02	−0.69	< 0.01
SAT mass	−0.29	0.10	−0.43	0.03

Values are normalized to total ELV protein levels in each sample. *P* values for correlations are based on Pearson or Spearman analysis (when the data are not normally distributed).

Abbreviations: Pho-Rictor/P = phosphorylated Rictor/protein, Omentin/P = Omentin-1/protein. WC = waist circumference; TG = triglyceride; FINS = fasting insulin; VAT = visceral fat; SAT = subcutaneous fat; FC-P/G = fasting C-peptide to Glucose Ratio; ISI-Matsuda = Matsuda index; AUC<sub>INS/G</sub> = Insulin secretion index.

The statistical significance was set as  $P < 0.05$ .

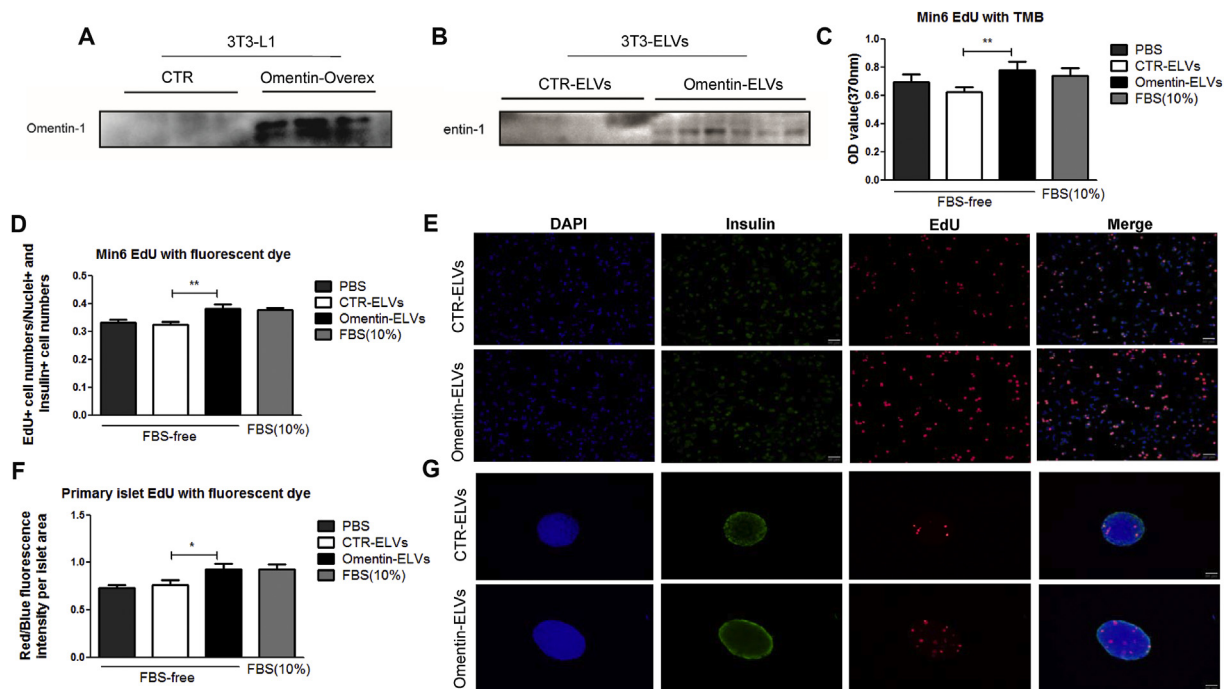


**Figure 6** Effect of Omentin-1-overexpressed ELVs on  $\beta$ -cell proliferation. 3T3-L1 preadipocytes were transfected with a plasmid containing the mouse Omentin-1 sequence (Omentin-Overex) or a control plasmid (CTR). 48 h after transfection, Omentin-1 protein expressions in cells (A) and released ELVs (B) were measured by Western blot. (C) Min6 cells (300 cells/well) were cultured in serum-free medium with 5  $\mu$ g/mL Omentin-1-enriched ELVs for overnight. EdU was added 2 h before cells were fixed and detected by TMB coloration. (D) Min6 cells ( $2 \times 10^5$  cells/well) were treated as in (C) and EdU was detected by fluorescent dye. Data were presented as a ratio (EdU<sup>+</sup> cell numbers/Nuclei<sup>+</sup> and Insulin<sup>+</sup> cell numbers). (E) Representative images (40x magnification) of the Min6 cells labeled with EdU (red), nuclei (blue), and insulin (green). (F) Primary islets were cultured in serum-free medium with 10  $\mu$ g/mL Omentin-1-enriched ELVs and EdU for 48 h. EdU was detected by fluorescent dye. Data were presented as a ratio (Red fluorescence intensity/Blue fluorescence intensity per islet area). (G) Representative images (20x magnification) of the islets labeled with EdU (red), nuclei (blue), and insulin (green). Under these serum-free conditions (C, D, F), serum containing medium (10% FBS) were used as a positive control. Results shown herein (C, D, F) are the means  $\pm$  SEM for 3 repeated experiments. CTR-ELVs: ELVs released from 3T3-L1 preadipocytes transfected with control plasmid. Omentin-ELVs: ELVs released from 3T3-L1 preadipocytes overexpressing Omentin-1. \* $P < 0.05$  vs. CTR-ELVs. \*\* $P < 0.01$  vs. CTR-ELVs.

pathway, has been shown to regulate  $\beta$ -cell proliferation, mass, and secretory function.<sup>29</sup> The activation of Rictor/mTORC2 declined in islets from patients with T2DM.<sup>30</sup> The specific knockout of Rictor in mouse  $\beta$ -cells caused a reduction in  $\beta$ -cell mass, proliferation, and insulin secretion due to locally decreased phosphorylation of Akt-S473 and increased cell cycle inhibitors (FOXO1 and p27).<sup>31</sup> Likewise,  $\beta$ -cell Rictor-specific-knockout mice on a high-fat diet exhibited blunted  $\beta$ -cell proliferation and restricted compensatory expansion of  $\beta$ -cell mass.<sup>32</sup> Another identified exosomal protein, Omentin-1, has been regarded as a new secretory adipokine since it is highly secreted by omental adipose tissue in humans. The circulating Omentin-1 levels were very high and decreased in obesity and insulin resistance.<sup>33</sup> Its implication in proliferation has also been evidenced that Omentin-1 promoted cellular proliferation in several cell types, including mesenchymal stem cells, neural stem cells, and osteoblast via the activation of PI3K/Akt signaling pathway.<sup>34–36</sup> Yet, the effect of Omentin-1 on  $\beta$ -cell proliferation has not been investigated. We validated

*in vitro* that ELV-carried Omentin-1 and Omentin-1 protein *per se* were indeed able to increase  $\beta$ -cell proliferation, Akt activity and protein levels of Cyclin D2(25). Moreover, Cyclin D2, the crucial cell cycle protein, which was down-regulated by circulating ELVs of subjects with simple obesity, was upregulated by Omentin-1-overexpressed ELVs. These findings suggested that the downregulated Omentin-1 cargo likely participated in the effect of circulating ELVs on impaired  $\beta$ -cell proliferation in nondiabetic obesity. Since  $\beta$ -cell proliferation was regulated by both positive and negative factors, our findings also indicated that the effect of ELVs on impaired  $\beta$ -cell proliferation was partly through the downregulation of positive factors. So far, the specific receptor for omentin-1 has not been identified. Studies suggest that the physiological activities of Omentin-1 might be not through a specific protein receptor. Thus, the ELV-carried form might be a pathway for Omentin-1 to act on cells. Moreover, compared to the free Omentin-1, the ELV-carried form of Omentin-1 would probably facilitate the application of this adipokine in the

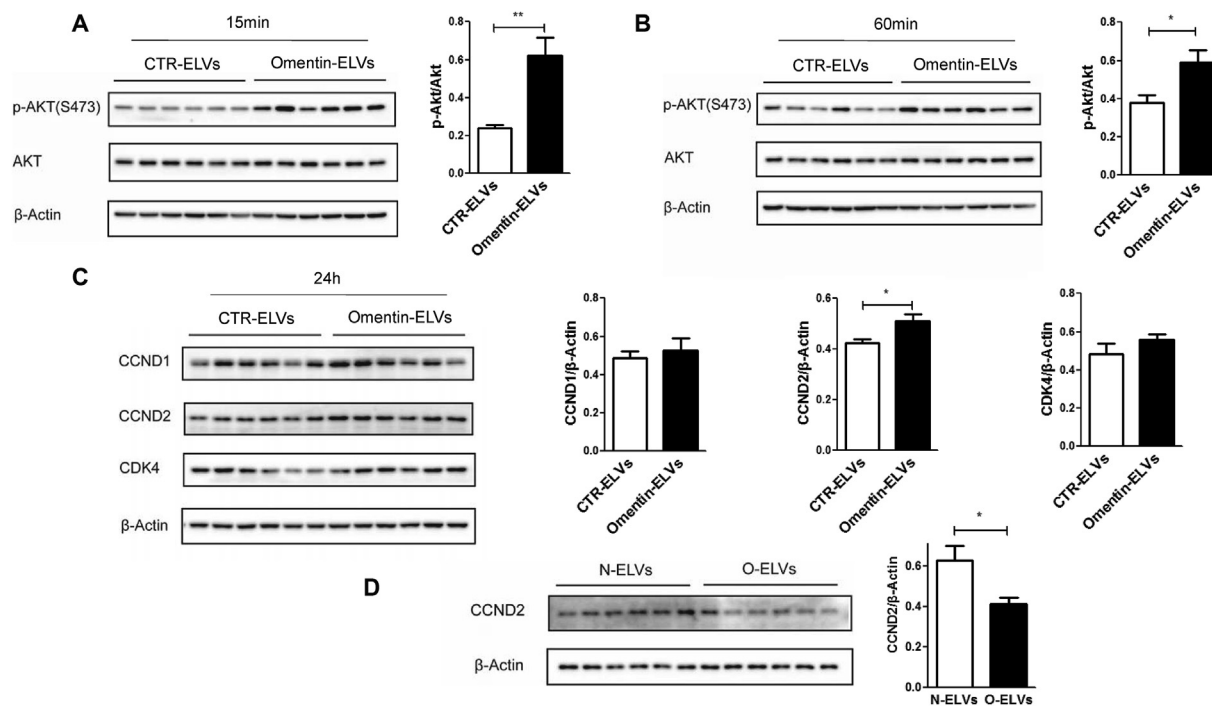


**Figure 7** Effect of Omentin-1-overexpressed ELVs on Akt activity and cell cycle proteins in  $\beta$ -cells. **(A, B)** Min6 cells were cultured in serum-free medium for overnight and treated with 5  $\mu\text{g}/\text{mL}$  ELVs for 15 and 60 min, respectively. Phosphorylation of Akt was measured by Western blot and normalized to total Akt protein levels. **(C)** Min6 cells were cultured in serum-free medium and treated with 5  $\mu\text{g}/\text{mL}$  ELVs for 24 h. Cyclin D1 (CCND1), Cyclin D2 (CCND2), and cyclin dependent kinase 4 (CDK4) were measured by Western blot. **(D)** Min6 cells were cultured in ELV-depleted medium and treated with 200  $\mu\text{g}/\text{mL}$  human ELVs for 48 h. CCND2 was measured by Western blot. Results shown herein (A–D) are the means  $\pm$  SEM for 3 repeated experiments. The representative blots are shown on the left. CTR-ELVs: ELVs released from 3T3-L1 preadipocytes transfected with control plasmid. Omentin-ELVs: ELVs released from 3T3-L1 preadipocytes overexpressing Omentin-1. N-ELVs: ELVs isolated from plasma of subjects with normal weight; O-ELVs: ELVs isolated from plasma of subjects with simple obesity. \* $P < 0.05$  vs. CTR-ELVs, \*\* $P < 0.01$  vs. CTR-ELVs.

treatment of disease as ELVs have been regarded as natural drug delivery tools.

Furthermore, we found that the decreased levels of Rictor and Omentin-1 in circulating ELVs were closely associated with abdominal obesity, hypertriglyceridemia, or hyperinsulinemia, suggesting that the ELV protein cargos could be modulated by obesity-related pathologic conditions. This hypothesis was partly supported by validating *in vitro* that Omentin-1 levels in human omental AT-released ELVs were actually downregulated by insulin treatment. It has been shown that insulin could directly stimulate  $\beta$ -cell proliferation *in vitro* and hyperinsulinemia was associated with increased  $\beta$ -cell mass *in vivo*.<sup>37,38</sup> Our results indicated that the hyperinsulinemia may serve as a *double-sided sword*, which could also potentially blunt  $\beta$ -cell proliferation via modulating cargos of ELVs. Thus, ELV-carried Omentin-1 might be a potential mediator linking insulin resistance (hyperinsulinemia) to impaired adaptive  $\beta$ -cell proliferation.

Taken together our data suggest that hyperinsulinemia in obesity could target visceral AT to downregulate the protein levels of Omentin-1 in AT-released ELVs, which go into circulation and deliver insufficient Omentin-1 in

recipient  $\beta$ -cells. This may lead to reduced activity of Akt and protein levels of Cyclin D2, thereby impairing  $\beta$ -cell proliferation (Fig. S6).

Finally, some limitations of this study should be mentioned. First, the cargos of ELVs are complex. We analyzed only the protein components of ELVs on account of the limited plasma sample of an individual. More components like miRNAs modulated in obesity needs to be identified. Second, we focused on validating the function of ELV-carried Omentin-1 in  $\beta$ -cell proliferation. The cell origins and functions of Rictor will be instrumental in further deciphering the effect of ELVs on  $\beta$ -cells. Third, we observed the phenotype and underlying mechanisms regulated by ELV-carried Omentin-1 *in vitro*, the phenotype and mechanisms *in vivo*, are warranted to be unraveled.

In conclusion, the circulating ELVs in nondiabetic obesity acted as a negative regulator for  $\beta$ -cell proliferation. Two protein cargos of circulating ELVs were identified to be downregulated by obesity-related pathologic conditions. The downregulated Omentin-1 protein was likely to participate in the effect of ELVs on impaired  $\beta$ -cell proliferation. Thus, the circulating ELV-carried Omentin-1 could

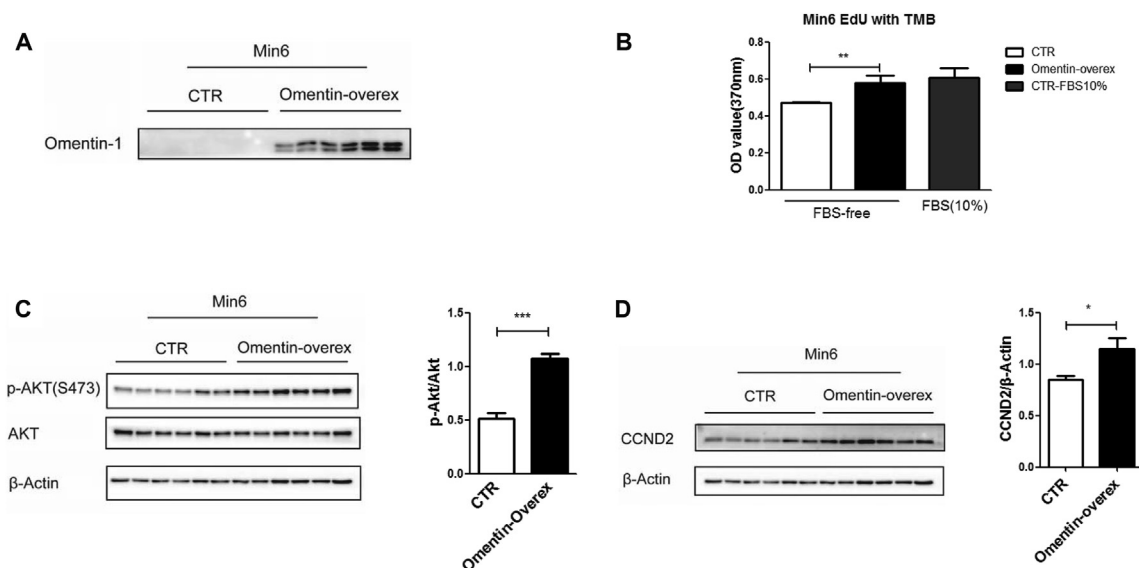


**Figure 8** Effect of Omentin-1 protein overexpression in  $\beta$ -cells on cellular proliferation. Min6 cells were transfected with a plasmid containing the mouse Omentin-1 sequence (Omentin-Overex) or a control plasmid (CTR) and cultured in serum-free medium. 48 h after transfection, cells were seeded for EdU detection or collected for Western blot. **(A)** Omentin-1 protein expressions in transfected cells were detected by Western blot. **(B)** Transfected cells (3000 cells/well) were seeded in a 96-well plate and cultured in serum-free medium for overnight. EdU was added 2 h before cells were fixed and detected by TMB coloration. **(C)** Phosphorylation of Akt in transfected cells was measured by Western blot and normalized to total Akt protein levels. **(D)** Protein levels of Cyclin D2 (CCND2) in transfected cells were measured by Western blot. Results shown herein (B–D) are the means  $\pm$  SEM for 3 repeated experiments. The representative blots are shown on the left. \* $P < 0.05$  vs. CTR, \*\*\* $P < 0.001$  vs. CTR.

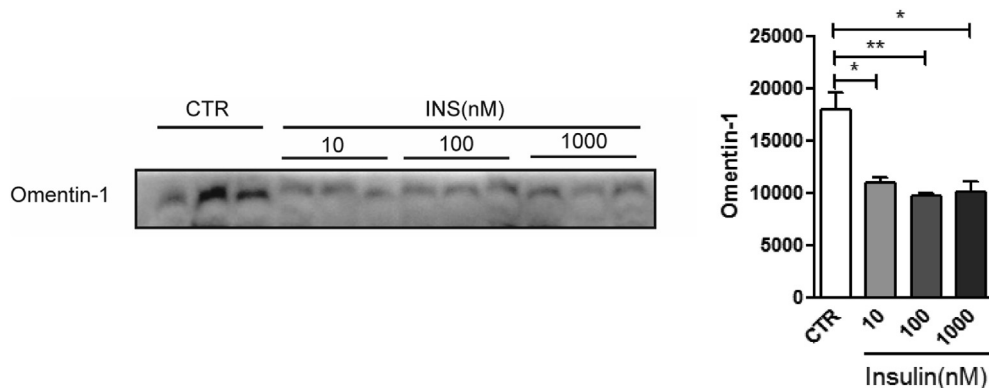


**Figure 9** Effect of insulin on Omentin-1 protein expression in ELVs released from human omental adipose tissues. Explants of human omental adipose tissues (AT) were cultured in ELV-depleted medium with or without insulin for 24 h. Omentin-1 in AT-released ELVs were detected by Western blot. A representative blot is shown on the left. Data are presented as the bound volumes. Results are means  $\pm$  SEM for 3 repeated experiments.

be a new potential target for increasing  $\beta$ -cell mass in obesity and T2DM.

## Author contributions

Pr. Xi Li and Xiaoqiu Xiao are the guarantors of this work, had full access to all the data and takes full responsibility for the integrity of data and the accuracy of data analysis. Qian Ge researched data, wrote the manuscript, contributed to discussion, and reviewed/edited manuscript. Xinxin Xie researched data, reviewed/edited the manuscript. Xiangjun Chen collected human plasma samples. Rongfeng

Huang raised mice. Cheng-Xue Rui taught the method for isolation and culture of primary islets. Qianna Zhen, Renzhi Hu and Min Wu assisted. Xi Li and Xiaoqiu Xiao contributed to discussion, reviewed/edited manuscript.

## Funding

This work was supported by the National Key R&D Program of China (No. 2018YFA0800401); the National Natural Science Foundation of China (No. 81200629, 81570763, 81770861 and 31571401); the Fundamental Science and Advanced Technology Research of Chongqing (Major

Project, No. CSTC2015jcyjB0146); the Chongqing Science and Technology Foundation (No. cstc2018jcyjAX0232); the Science and Technology Research Program of Chongqing Municipal Education Commission (No. KJZD-K201800402).

## Data availability

The datasets generated during and/or analyzed during the current study are available from the corresponding author on reasonable request.

## Conflict of interests

The authors declared no conflict of interest.

## Acknowledgements

We thank the Hepatobiliary Surgery Department of the First Affiliated hospital of Chongqing Medical University for the preparation of human omental adipose tissue.

## Appendix A. Supplementary data

Supplementary data to this article can be found online at <https://doi.org/10.1016/j.gendis.2020.12.011>.

## References

- Pan J, Jia W. Early-onset diabetes: an epidemic in China. *Front Med*. 2018;12(6):624–633.
- Prentki M, Nolan CJ. Islet beta cell failure in type 2 diabetes. *J Clin Invest*. 2006;116(7):1802–1812.
- Linnemann AK, Baan M, Davis DB. Pancreatic beta-cell proliferation in obesity. *Adv Nutr*. 2014;5(3):278–288.
- El Ouaamari A, Dirice E, Gedeon N, et al. SerpinB1 promotes pancreatic beta cell proliferation. *Cell Metab*. 2016;23(1):194–205.
- Farooqi AA, Desai NN, Qureshi MZ, et al. Exosome biogenesis, bioactivities and functions as new delivery systems of natural compounds. *Biotechnol Adv*. 2018;36(1):328–334.
- Ge Q, Xie XX, Xiao X, Li X. Exosome-like vesicles as new mediators and therapeutic targets for treating insulin resistance and beta-cell mass failure in type 2 diabetes mellitus. *J Diabetes Res*. 2019;2019:3256060.
- Jalabert A, Vial G, Guay C, et al. Exosome-like vesicles released from lipid-induced insulin-resistant muscles modulate gene expression and proliferation of beta recipient cells in mice. *Diabetologia*. 2016;59(5):1049–1058.
- Tsukita S, Yamada T, Takahashi K, et al. MicroRNAs 106b and 222 improve hyperglycemia in a mouse model of insulin-deficient diabetes via pancreatic beta-cell proliferation. *EBioMedicine*. 2017;15:163–172.
- Guay C, Menoud V, Rome S, Regazzi R. Horizontal transfer of exosomal microRNAs transduce apoptotic signals between pancreatic beta-cells. *Cell Commun Signal*. 2015;13(1):17.
- Chen C, Lu FC, Department of Disease Control Ministry of Health PRC. The guidelines for prevention and control of overweight and obesity in Chinese adults. *Biomed Environ Sci*. 2004;17(Suppl):1–36.
- Zhen Q, Yao N, Chen X, Zhang X, Wang Z, Ge Q. Total body adiposity, triglycerides, and leg fat are independent risk factors for diabetic peripheral neuropathy in Chinese patients with type 2 diabetes mellitus. *Endocr Pract*. 2019;25(3):270–278.
- Liu L, Li Q, Xiao X, et al. miR-1934, downregulated in obesity, protects against low-grade inflammation in adipocytes. *Mol Cell Endocrinol*. 2016;428:109–117.
- Mincheva-Nilsson L, Baranov V, Nagaeva O, Dehlin E. Isolation and characterization of exosomes from cultures of tissue explants and cell lines. *Curr Protoc Immunol*. 2016;115:14.42.1-14.42.21.
- Du ZY, Ma T, Lock EJ, et al. Depot-dependent effects of adipose tissue explants on co-cultured hepatocytes. *PLoS One*. 2011;6(6):e20917.
- Ge Q, Ryken L, Noel L, Maury E, Brichard SM. Adipokines identified as new downstream targets for adiponectin: lessons from adiponectin-overexpressing or -deficient mice. *Am J Physiol Endocrinol Metab*. 2011;301(2):E326–E335.
- Guo X, Zhang Z, Zeng T, et al. cAMP-MicroRNA-203-IFN $\gamma$  network regulates subcutaneous white fat browning and glucose tolerance. *Mol Metab*. 2019;28:36–47.
- Li L, Li C, Wang S, et al. Exosomes derived from hypoxic oral squamous cell carcinoma cells deliver miR-21 to normoxic cells to elicit a prometastatic phenotype. *Cancer Res*. 2016;76(7):1770–1780.
- Tang N, Sun B, Gupta A, Rempel H, Pulliam L. Monocyte exosomes induce adhesion molecules and cytokines via activation of NF- $\kappa$ B in endothelial cells. *FASEB J*. 2016;30(9):3097–3106.
- Lotvall J, Hill AF, Hochberg F, et al. Minimal experimental requirements for definition of extracellular vesicles and their functions: a position statement from the International Society for Extracellular Vesicles. *J Extracell Vesicles*. 2014;3(1):26913.
- Mulcahy LA, Pink RC, Carter DR. Routes and mechanisms of extracellular vesicle uptake. *J Extracell Vesicles*. 2014;3:24641.
- Eguchi K, Nagai R. Islet inflammation in type 2 diabetes and physiology. *J Clin Invest*. 2017;127(1):14–23.
- Yang H, Rudge DG, Koos JD, Vaidialingam B, Yang HJ, Pavletich NP. mTOR kinase structure, mechanism and regulation. *Nature*. 2013;497(7448):217–223.
- Watanabe T, Watanabe-Kominato K, Takahashi Y, Kojima M, Watanabe R. Adipose tissue-derived omentin-1 function and regulation. *Compr Physiol*. 2017;7(3):765–781.
- Saisho Y. Postprandial C-peptide to glucose ratio as a marker of beta cell function: implication for the management of type 2 diabetes. *Int J Mol Sci*. 2016;17(5):744.
- Kulkarni RN, Mizrachi EB, Ocana AG, Stewart AF. Human beta-cell proliferation and intracellular signaling: driving in the dark without a road map. *Diabetes*. 2012;61(9):2205–2213.
- Fatrai S, Elghazi L, Balcazar N, et al. Akt induces beta-cell proliferation by regulating cyclin D1, cyclin D2, and p21 levels and cyclin-dependent kinase-4 activity. *Diabetes*. 2006;55(2):318–325.
- Ji Y, Sun S, Shrestha N, et al. Toll-like receptors TLR2 and TLR4 block the replication of pancreatic beta cells in diet-induced obesity. *Nat Immunol*. 2019;20(6):677–686.
- Carboneau BA, Allan JA, Townsend SE, Kimple ME, Breyer RM, Gannon M. Opposing effects of prostaglandin E2 receptors EP3 and EP4 on mouse and human beta-cell survival and proliferation. *Mol Metab*. 2017;6(6):548–559.

29. Yuan T, Lupse B, Maedler K, Ardestani A. mTORC2 signaling: a path for pancreatic beta cell's growth and function. *J Mol Biol*. 2018;430(7):904–918.
30. Yuan T, Rafizadeh S, Gorrepati KD, et al. Reciprocal regulation of mTOR complexes in pancreatic islets from humans with type 2 diabetes. *Diabetologia*. 2017;60(4):668–678.
31. Gu Y, Lindner J, Kumar A, Yuan W, Magnuson MA. Rictor/mTORC2 is essential for maintaining a balance between beta-cell proliferation and cell size. *Diabetes*. 2011;60(3):827–837.
32. Xie Y, Cui C, Nie A, et al. The mTORC2/PKC pathway sustains compensatory insulin secretion of pancreatic beta cells in response to metabolic stress. *Biochim Biophys Acta Gen Subj*. 2017;1861(8):2039–2047.
33. de Souza Batista CM, Yang RZ, Lee MJ, et al. Omentin plasma levels and gene expression are decreased in obesity. *Diabetes*. 2007;56(6):1655–1661.
34. Zhao LR, Du YJ, Chen L, et al. Omentin-1 promotes the growth of neural stem cells via activation of Akt signaling. *Mol Med Rep*. 2015;11(3):1859–1864.
35. Yin L, Huang D, Liu X, et al. Omentin-1 effects on mesenchymal stem cells: proliferation, apoptosis, and angiogenesis in vitro. *Stem Cell Res Ther*. 2017;8(1):224.
36. Wu SS, Liang QH, Liu Y, Cui RR, Yuan LQ, Liao EY. Omentin-1 stimulates human osteoblast proliferation through PI3K/Akt signal pathway. *Internet J Endocrinol*. 2013;2013:368970.
37. Wang Q, Jin T. The role of insulin signaling in the development of beta-cell dysfunction and diabetes. *Islets*. 2009;1(2):95–101.
38. Beith JL, Alejandro EU, Johnson JD. Insulin stimulates primary beta-cell proliferation via Raf-1 kinase. *Endocrinology*. 2008;149(5):2251–2260.